

# Blending NPP-VIIRS and Landsat OLI Images for Flood Inundation Monitoring

**C. Huang**<sup>a</sup>, **Y. Chen**<sup>b</sup>, **S.Q. Zhang**<sup>a</sup>, **R. Liu**<sup>c</sup>, **K.F. Shi**<sup>c</sup>, **L.Y. Li**<sup>d</sup> and **J.P. Wu**<sup>c</sup>

<sup>a</sup> College of Urban and Environmental Sciences, Northwest University, Xi'an 710127, China

<sup>b</sup> CSIRO Land and Water, Canberra, ACT 2601, Australia

<sup>c</sup> Key Laboratory of Geographic Information Science, Ministry of Education, East China Normal University, Shanghai 200241, China

<sup>d</sup> School of Remote Sensing and Information Engineering, Wuhan University, Wuhan 430079, China

Email: [changh@nwu.edu.cn](mailto:changh@nwu.edu.cn)

**Abstract:** Measuring surface water using remote sensing technology is an essential research topic in many research areas, including flood-related studies and water resource management. Recent advances in satellite remote sensing have provided more efficient ways of monitoring surface water from space. Several sensors, such as the Visible Infrared Imaging Radiometer Suite on board Suomi National Polar-orbiting Partnership (Suomi NPP-VIIRS) and Operational Land Imager (OLI) on board Landsat 8, have begun to monitor earth surface in recent years. They have been continuously providing enormous remotely sensed images. Nevertheless, it has to be noted that tradeoffs between spatial and temporal resolutions of these images still exist. Medium- to high-resolution images, such as Landsat OLI, are typically available fortnightly or less often, which limits their applications for intensively and continuously monitoring flood inundation dynamics. Whereas coarse-resolution sensors, such as NPP-VIIRS, scan the earth's surface once or several times a day, but their coarse spatial resolution hampers the correct mapping of flooded areas. This study, therefore, aims to blend NPP-VIIRS and Landsat OLI images in order to gain high spatial resolution from Landsat OLI and high temporal resolution from NPP-VIIRS simultaneously. Two classic fusion models, namely the Spatial and Temporal Adaptive Reflectance Fusion Model (STARFM) and the Enhanced Spatial and Temporal Adaptive Reflectance Fusion Model (ESTARFM) were tested and evaluated. Particularly, the fusion results of both models were compared with the actual Landsat images in order to evaluate the accuracy of these fusion results. It is hoped that this study will enlighten other studies that require remotely sensed data with both high spatial and temporal resolutions.

**Keywords:** *Surface water, image fusion, image blending, Spatial and Temporal Adaptive Reflectance Fusion Model (STARFM), Enhanced Spatial and Temporal Adaptive Reflectance Fusion Model (ESTARFM)*

## 1. INTRODUCTION

Flood is one of the common natural phenomena in many regions. In recent decades, due to the global warming and urbanization, flood has become even more frequent and harmful. Monitoring the inundation caused by flood is thus crucial, for many flood-related studies (Chen *et al.*, 2015; Wang *et al.*, 2015).

Due to its efficiency, remote sensing has become a widely used technique in flood inundation monitoring. A variety of related studies have been performed since the 1970s. Optical sensors, such as Landsat Multispectral Scanner (MSS) and Thematic Mapper (TM)/Enhanced Thematic Mapper Plus (ETM+) (Rango and Salomonson, 1974; Chen *et al.*, 2014), NOAA Advanced Very High Resolution Radiometer (AVHRR) (Barton and Bathols, 1989; Jain *et al.*, 2006), and Moderate Resolution Imaging Spectroradiometer (MODIS) (Chen *et al.*, 2013; Huang *et al.*, 2014a; Ticehurst *et al.*, 2014; Liu *et al.*, 2015), have been widely applied in flood inundation monitoring. Recent advances in satellite remote sensing promise more accurate monitoring of flood inundation. Operational Land Imager (OLI) on board the Landsat 8, which has a spatial resolution of 30m, was considered as a continuation and improvement of ETM+. Its potential applications in flood inundation monitoring are enormous. Another satellite mission, the Suomi National Polar-orbiting Partnership (Suomi NPP), is a new generation of satellites intended to replace the Earth Observing System satellites (Shi *et al.*, 2014). The Visible Infrared Imaging Radiometer Suite (VIIRS) that is onboard provides a range of visible and infrared bands (spatial resolution ranging from 375m to 750m) to observe the earth's surface. It is considered as an upgrade and replacement of the AVHRR and MODIS as a wide-swath multispectral sensor (Yu *et al.*, 2005). The capability of NPP-VIIRS in surface water detection has been proven (Huang *et al.*, 2015). It is promising that it can be widely applied in monitoring flood inundation in the near future.

There is a general consensus that a trade-off exists between the spatial and temporal resolution of the aforementioned optical sensors (Huang *et al.*, 2014b; Li *et al.*, 2015a; Li *et al.*, 2015b). Medium- to high-resolution images, such as Landsat OLI, are typically available fortnightly or less often, which limits their application in intensively and continuously monitoring flood inundation. Whereas coarse-resolution sensors, such as NPP-VIIRS, scan the earth's surface once or several times a day, but they have coarse spatial resolution, which hampers the accurate mapping of inundated areas.

Data fusion (or blending) is a technique that aims to exploit more information by integrating various data (Pohl and Van Genderen, 1998). This has been proven to be a feasible solution for the spatial and temporal trade-off issue. Gao *et al.* (2006) developed a Spatial and Temporal Adaptive Reflectance Fusion Model (STARFM) to generate a new Landsat-like image from a MODIS image on the same day by computing and modelling spectral, temporal, and spatial differences in the base images from Landsat and MODIS. Zhu *et al.* (2010) modified the model by taking into account the spatial heterogeneity within mixed pixels, and presented a new model named Enhanced Spatial and Temporal Adaptive Reflectance Fusion Model (ESTARFM). However, it is not ascertain that ESTARFM surpasses STARFM in different cases. Actually, the performance of blending methods is strongly related to the spatial and temporal condition of land covers (Emelyanova *et al.*, 2013). Besides, existing studies focus on blending Landsat and MODIS. It is necessary to test the effectiveness of the two models in the fusion of Landsat OLI and NPP-VIIRS for flood inundation monitoring. As it is well-known, Short-Wave Infrared (SWIR) band is a most sensitive channel for flood detection, and it has been used in water indices that are widely implemented in surface water detection and flood monitoring studies (Xu, 2006; Ji *et al.*, 2009; Li *et al.*, 2013).

The aim of this study, therefore, is to conduct an elementary and exploratory experiment to blend the SWIR bands of Landsat OLI and NPP-VIIRS. Two popular models, namely STARFM and ESTARFM, were chosen to generate a 30m resolution Landsat-like image with multiple combinations of Landsat OLI and NPP-VIIRS datasets. Blending results were then compared with the actual Landsat SWIR band on the same day, the difference of which was then considered as an essential index of the effectiveness of blending models.

## 2. STUDY AREA AND MATERIALS

### 2.1. Study area

The study area (Figure 1) is located in the southern part of Zhejiang province, China. It covers an area of 30,000×30,000 m<sup>2</sup> in the majority of Lishui which is a prefecture-level city of Zhejiang. Oujiang River is a major river that goes through Lishui city. A section of Oujiang River is also included in the study area. On 20

August 2014, Lishui suffered a 1-in-50 flood. A majority of the city was flooded and more than 30,000 people were affected.



**Figure 1.** Study area and its location.

## 2.2. Data

In this study, three pairs of cloud-free Landsat images and NPP-VIIRS images (acquired on 3 May 2014, 22 July 2014, and 26 October 2014) were collected to test the performance of both STARFM and ESTARFM. The time lags between these three pairs of images are all less than 4 hours. Band 6 of Landsat OLI (wavelength from 1.57-1.65 $\mu\text{m}$ ) and Imagery-resolution Band 3 (I3) of NPP-VIIRS (wavelength from 1.58-1.64 $\mu\text{m}$ ) were employed as the input SWIR bands for the fusion models (Figure 2). Landsat OLI images were downloaded from Geospatial Data Cloud, Computer Network Information Center, CAS (<http://www.gscloud.cn>). NPP-VIIRS images were downloaded from NOAA/Comprehensive Large Array-Data Stewardship System (<http://www.nsof.class.noaa.gov/>). Both coarse-resolution and fine-resolution images need to be processed geometrically and radiometrically before blending. All images were calibrated to reflectance to make them comparable and consistent. After that, the 375m resolution NPP-VIIRS images were reprojected to the same projection as Landsat images, and resampled to 30m resolution. Each pair of Landsat image and resampled NPP-VIIRS image was precisely registered.

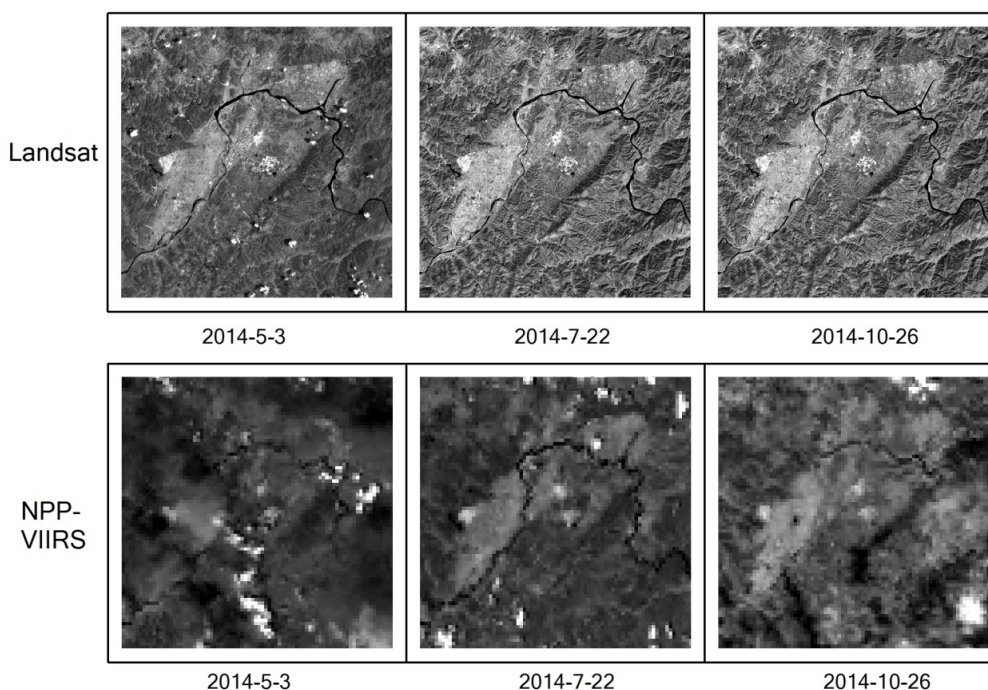


**Figure 2.** Three pairs of SWIR bands of Landsat and NPP-VIIRS.

### 3. FUSION MODELS

#### 3.1. Spatial and Temporal Adaptive Reflectance Fusion Model (STARFM)

The assumption of STARFM is that Landsat and MODIS surface reflectance data on the same day are consistently related to each other (Gao *et al.*, 2006). Under this assumption, this method tries to predict synthetic images at time  $t_2$  by fusing a Landsat image at time  $t_1$  and two MODIS images at both time  $t_1$  and time  $t_2$ . It mainly consists of three steps. The first step is to select spectrally similar pixels from Landsat image based on a predefined size of moving window; the second is to determine a weighting function for both Landsat and MODIS images and calculate a weighted factor for each moving window; and the last is to generate the synthetic Landsat images at time  $t_2$  by multiplying the weighted factor with the sum of difference between two MODIS images taken at two different times and Landsat image at time  $t_1$ .

There are two major issues that might affect the fusion result of STARFM. The first one is that the moving window size is variable depending on the study area. Therefore it has to be determined carefully for different study areas. The second one is that this model does not work properly over heterogeneous land cover types (Zhu *et al.*, 2010).

#### 3.2. Enhanced Spatial and Temporal Adaptive Reflectance Fusion Model (ESTARFM)

In order to achieve more accurate prediction of surface reflectance in heterogeneous landscapes, Zhu *et al.* (2010) proposed an enhanced STARFM (ESTARFM) method. It improves on the original algorithm by using the observed reflectance trend between two points in time, and spectral unmixing theory. Therefore, for the ESTARFM, at least one more pair of Landsat and MODIS images at another time phase was needed.

For instance, three MODIS images at three time phases ( $t_1$ ,  $t_2$  and  $t_3$ ) and Landsat images at two time phases ( $t_1$  and  $t_3$ ) can be used to predict a synthetic Landsat-like image at time  $t_2$  using ESTARFM. It mainly involves four steps. The first two steps are the same as STARFM. The third step is to determine a conversion coefficient for each similar pixel by linear regression of two pairs of corresponding Landsat and MODIS images (i.e.  $t_1$  and  $t_3$ ). The last step is to generate synthetic image for  $t_2$  by integrating the outcomes of the weighted factor, the conversion coefficient and MODIS image of time  $t_2$ .

### 4. RESULTS AND DISCUSSION

In this study, the SWIR band of NPP-VIIRS was used to replace the MODIS images in the original STARFM and ESTARFM algorithms. Figure 3(a) and 3(b) show the predicted surface reflectance images on 26 October 2014 from both models, in comparison with the corresponding reflectance from the actual Landsat SWIR band on the same day (Figure 3(c)). The SWIR band of NPP-VIIRS on the same day (Figure 3(d)), which is an important input of the fusion models, was also presented for reference.

It is clear from Figure 3 that both predicted reflectance results have a finer spatial resolution than the NPP-VIIRS band. Land cover information is presented in a more detailed way. Rivers, even small rivers, can be clearly observed from the fusion result. However, it is also obvious that although the fusion results have the same spatial resolution as the actual Landsat, they cannot exhibit land cover information as exquisite as the actual Landsat does. Delicate terrain information has not been properly restored. Relatively speaking, ESTARFM-predicted result is slightly better than that of STARFM-predicted. Terrain texture has been preserved in some areas in the ESTARFM-predicted result. Moreover, both results have been affected by the cloud cover in the input images. For example, the high reflectance areas (as shown in red circles in Figure 3(a) and (b)) in the predicted results were introduced by the cloud cover in the input NPP-VIIRS image (as shown in red circles in Figure 3(d)). Some unusual low reflectance areas (as shown in blue ellipse in Figure 3(a) and (b)) were also introduced by the cloud cover in the input images of the fusion models (can be identified in NPP-VIIRS of 3 May 2014 in Figure 2). Generally speaking, if the cloud cover happened on the earlier time phase, it would cause underestimation of reflectance. If it happened on the later time phase, it would overestimate the surface reflectance.

In order to quantitatively assess the accuracy of the fusion results, both predicted reflectance images were compared with the actual Landsat SWIR band on the same day on a pixel-by-pixel basis. Scatter plots in Figure 4 show the relationship of reflectance between the predicted and actual values. It can be seen from Figure 4 that both plots are almost the same. Most of the data in the scatter plots fall close to the 1:1 line, indicating that both fusion models can predict the surface reflectance reasonably. It is also noted that some pixels have obvious difference on the predicted reflectance and actual reflectance. By cross checking with Figure 3, it was found that most of these pixels were affected by cloud cover, either at the earlier time phase

or the later. Root Mean Square Deviation (RMSD) was also calculated for both comparisons. The RMSD between the STARFM-predicted reflectance and actual Landsat reflectance is 0.078, while the RMSD between the ESTARFM-predicted reactance and actual Landsat reflectance is 0.074, indicating a slightly better prediction than the STARFM method.

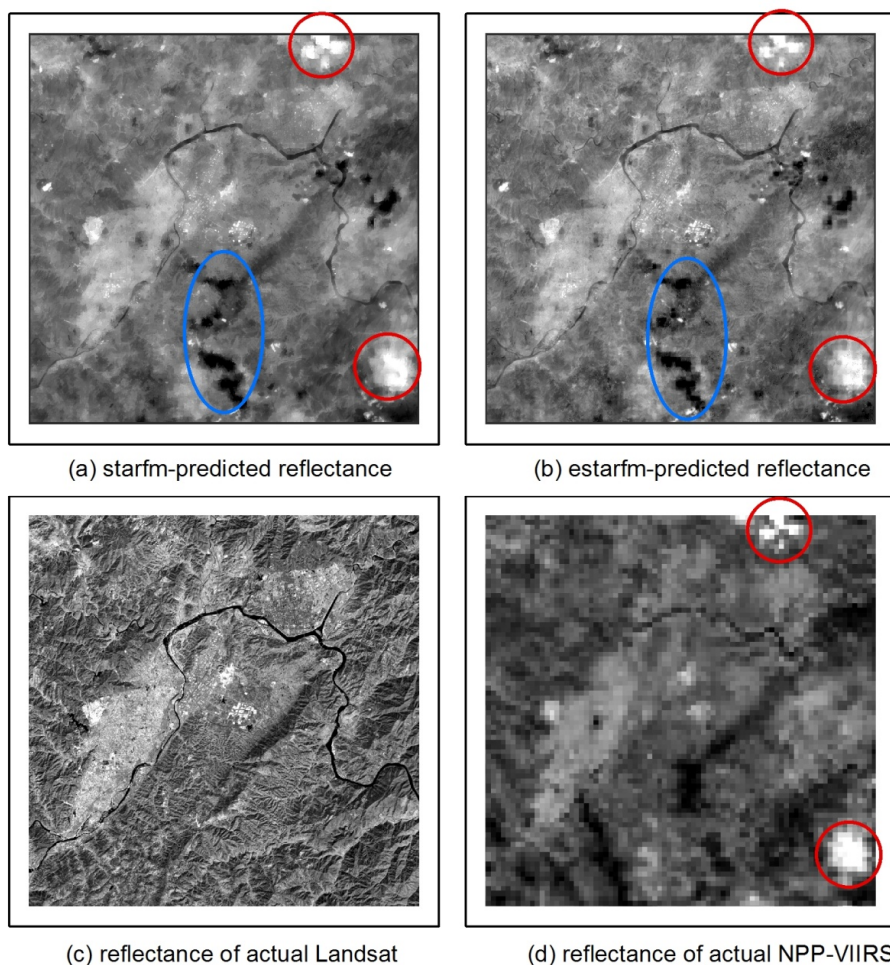


**Figure 3.** Predicted surface reflectance on 26 October 2014 from STARFM and ESTARFM, along with the actual Landsat reflectance and NPP-VIIRS reflectance on the same day.

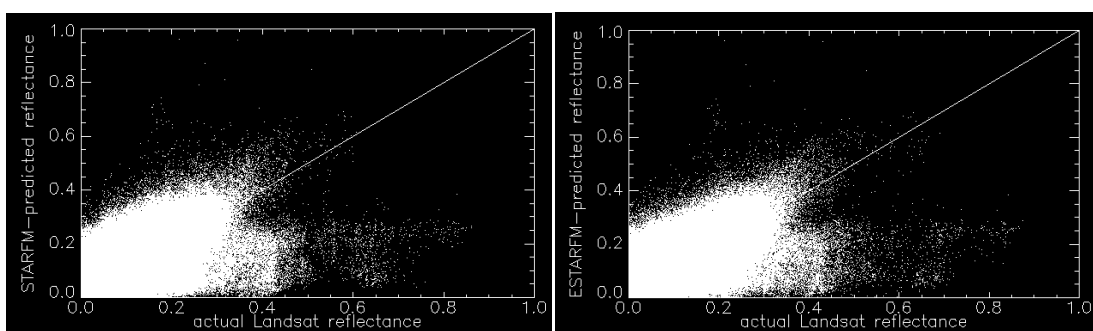


**Figure 4.** Scatter plots of STARFM-predicted and actual Landsat reflectance (left), ESTARFM-predicted and actual Landsat reflectance (right).

## 5. CONCLUSION

Flood monitoring with remotely sensed imagery usually requires both high spatial and temporal resolutions, which originally cannot be achieved for a single type of sensor. Image fusion is an effective way to blend different types of satellite imagery and acquire their advantages in either spatial or temporal resolutions. Three pairs of Landsat and NPP-VIIRS images were applied to test two popular blending models (i.e.

STARFM and ESTARFM) in a flooding event of Lishui in 2014. Results demonstrated the differing capability of these two models in the prediction of surface reflectance. Both models share some similarities in predicting surface reflectance. High spatial resolution can be achieved and detailed land cover information can be restored based on the available limited number of fine-resolution and coarse-resolution images. Evaluation results reveal that fusion results of both models were acceptable. The difference between the modeled reflectance and actual reflectance is less than 0.08. Generally speaking, ESTARFM derived a slightly better result than STARFM did.

As this is an elementary and exploratory blending experiment, there are several limitations that need to be addressed in the future study. First, only SWIR band was tested for blending in this study. Although SWIR band is sensitive to surface water and flood detection, a single SWIR band is not enough for an accurate detection, more bands should be investigated. Second, cloud cover is also a big issue for image fusion. It seriously affects the fusion result. Therefore, integrating cloud identification and removal procedure into the fusion framework will be the subject of our future work.

## ACKNOWLEDGMENTS

This study is supported by National Major Scientific Research Program [Grant No. 2013CBA01806], the Special Trade Project for Commonwealth of Water Resources [Grant No. 201401026], National Natural Science Foundation of China [Grant No. 41501460] and Shanxi Key Science and Technology Innovation Team [Grant No. 2014KCT-27].

## REFERENCES

- Barton, I.J., and Bathols, J.M. (1989). Monitoring floods with AVHRR. *Remote Sensing of Environment*, 30(1): 89-94.
- Chen, Y., Huang, C., Ticehurst, C., Merrin, L., and Thew, P. (2013). An Evaluation of MODIS Daily and 8-day Composite Products for Floodplain and Wetland Inundation Mapping. *Wetlands*, 33(5): 823-835.
- Chen, Y., Liu, R., Barrett, D., Gao, L., Zhou, M., Renzullo, L. and Emelyanova, I. (2015). A spatial framework for evaluating regional-scale flooding risk under extreme climates. *Science of the Total Environment* (Accepted)
- Chen, Y., Wang B., Pollino, C.A., Cuddy, S.M., Merrin, L.E., and Huang, C., (2014). Estimate of flood inundation and retention on wetlands using remote sensing and GIS. *Ecohydrology*, 7: 1412-1420.
- Emelyanova, I.V., Movicar, T.R., Van Niel, T.G., LI, L.T., and Van Dijk, A.I.J.M. (2013). Assessing the accuracy of blending Landsat–MODIS surface reflectances in two landscapes with contrasting spatial and temporal dynamics: A framework for algorithm selection. *Remote Sensing of Environment*, 133(0): 193-209.
- Gao, F., Masek, J., Schwaller, M., and Hall, F. (2006). On the blending of the Landsat and MODIS surface reflectance: Predicting daily Landsat surface reflectance. *IEEE Transactions on Geoscience and Remote Sensing*, 44(8): 2207-2218.
- Huang, C., Chen, Y., and Wu, J. (2014a). Mapping spatio-temporal flood inundation dynamics at large river basin scale using time-series flow data and MODIS imagery. *International Journal of Applied Earth Observation and Geoinformation*, 26(0): 350-362.
- Huang, C., Chen, Y., Wu, J., Li, L., and Liu, R. (2015). An Evaluation of Suomi NPP-VIIRS Data for Surface Water Detection. *Remote Sensing Letters*, 6(2): 155-164.
- Huang, C., Chen, Y., and Wu, J. (2014b). DEM-based modification of pixel-swapping algorithm for enhancing floodplain inundation mapping. *International Journal of Remote Sensing*, 35(1): 365-381.
- Jain, S.K., Saraf, A.K., Goswami, A., and Ahmad, T. (2006). Flood inundation mapping using NOAA AVHRR data. *Water Resource Management*, 20(6): 949-959.
- Ji, L., Zhang, L., and Wylie, B. (2009). Analysis of Dynamic Thresholds for the Normalized Difference Water Index. *Photogrammetric Engineering and Remote Sensing*, 75(11): 1307-1317.
- Li, L., Chen, Y., Yu, X., Liu, R., and Huang, C. (2015a). Sub-pixel flood inundation mapping from multispectral remotely sensed images based on discrete particle swarm optimization. *ISPRS Journal of Photogrammetry and Remote Sensing*, 101(0): 10-21.

- Li, L., Chen, Y., Xu T., Liu, R, Shi, K., and Huang, C. (2015b). Super-resolution mapping of wetland inundation from remote sensing imagery based on integration of back-propagation neural network and genetic algorithm. *Remote Sensing of Environment*, 164:142–154.
- Li, S., Sun, D., Yu, Y., Csiszar, I., Stefanidis, A., and Goldberg, M.D. (2013). A New Short-Wave Infrared (SWIR) Method for Quantitative Water Fraction Derivation and Evaluation With EOS/MODIS and Landsat/TM Data. *IEEE Transactions on Geoscience and Remote Sensing*, 51(3): 1852-1862.
- Liu, R., Chen, Y., Wu, J., Gao, L., Barrett, D., Li, L., Huang, C., and Yu, j. (2015). Assessing spatial likelihood of flooding hazard using naïve Bayes and GIS - A case study in Bowen Basin, Australia. *Stochastic Environmental Research and Risk Assessment*, (in revised)
- Pohl, C., and Van Genderen, J.L. (1998). Review article Multisensor image fusion in remote sensing: Concepts, methods and applications. *International Journal of Remote Sensing*, 19(5): 823-854.
- Rango, A., and Salomonson, V.V. (1974). Regional flood mapping from space. *Water Resources Research*, 10(3): 473-484.
- Shi, K., Huang, C., Yu, B., Yin, B., Huang, Y., and Wu, J. (2014). Evaluation of NPP-VIIRS night-time light composite data for extracting built-up urban areas. *Remote Sensing Letters*, 5(4): 358-366.
- Ticehurst, C., Guerschman, J.P. and Chen, Y. (2014). The Strengths and limitations in using the daily MODIS Open Water Likelihood algorithm for identifying flood events. *Remote Sensing*, 6:11791-11809.
- Wang, B., Chen, Y., and Lu, C. (2015). Evaluating flood inundation impact on wetland vegetation FPAR of the Macquarie Marshes, Australia. *Environmental Earth Sciences*,
- Xu, H.Q. (2006). Modification of normalised difference water index (NDWI) to enhance open water features in remotely sensed imagery. *International Journal of Remote Sensing*, 27(14): 3025-3033.
- Yu, Y., Privette, J.L., and Pinheiro, A.C. (2005). Analysis of the NPOESS VIIRS Land Surface Temperature Algorithm Using MODIS Data. *IEEE Transactions on Geoscience and Remote Sensing*, 43 (10): 2340–2350.
- Zhu, X., Chen, J., Gao, F., Chen, X., and Masek, J.G. (2010). An enhanced spatial and temporal adaptive reflectance fusion model for complex heterogeneous regions. *Remote Sensing of Environment*, 114(11): 2610-2623.